Reevaluation of the parton distribution of strange quarks in the nucleon

A. Airapetian,[13,16] N. Akopov,[27] Z. Akopov,[6] E. C. Aschenauer,[7,*] W. Augustyniak,[26] A. Avetissian,[27] E. Avetisyan,[6] S. Belostotski,[19] H. P. Blok,[18,25] A. Borissov,[6] V. Bryzgalov,[20] J. Burns,[14] M. Capiluppi,[10] G. P. Capitani,[11] E. Cisbani,[22] G. Ciullo,[10] M. Contalbrigo,[10] P. F. Dalpiaz,[10] W. Deconinck,[6] R. De Leo,[2] E. De Sanctis,[11] M. Diefenthaler,[15,9] P. Di Nezza,[11] M. Düren,[13] M. Ehrenfried,[13] G. Elbakian,[27] F. Ellinghaus,[5] E. Etzelmüller,[13] L. Felawka,[23] S. Frullani,[22] D. Gabbert,[7] G. Gapienko,[20] V. Gapienko,[20] J. Garay García,[6,4] F. Garibaldi,[22] G. Gavrilov,[6,19,23] V. Gharibyan,[27] F. Giordano,[15,10] S. Gliske,[16] M. Hartig,[6] D. Hasch,[11] M. Hoek,[14] Y. Holler,[6] I. Hristova,[7] A. Ivanilov,[20] H. E. Jackson,[1] S. Joosten,[15,12] R. Kaiser,[14] G. Karyan,[27] T. Keri,[14,13] E. Kinney,[5] A. Kisselev,[19] V. Korotkov,[20] V. Kozlov,[17] P. Kravchenko,[19] V. G. Krivokhijine,[8] L. Lagamba,[2] L. Lapikás,[18] I. Lehmann,[14] P. Lenisa,[10] W. Lorenzon,[16] X.-G. Lu,[6] B.-Q. Ma,[3] D. Mahon,[14] S. I. Manaenkov,[19] Y. Mao,[3] B. Marianski,[26] H. Marukyan,[27] Y. Miyachi,[24] A. Movsisyan,[10,27] V. Muccifora,[11] M. Murray,[14] A. Mussgiller,[6,9] Y. Naryshkin,[19] A. Nass,[9] M. Negodaev,[7] W.-D. Nowak,[7] L. L. Pappalardo,[10] R. Perez-Benito,[13] A. Petrosyan,[27] P. E. Reimer,[1] A. R. Reolon,[11] C. Riedl,[15,7] K. Rith,[9] G. Rosner,[14] A. Rostomyan,[6] J. Rubin,[15] D. Ryckbosch,[12] Y. Salomatin,[20] A. Schäfer,[21] G. Schnell,[4,12] B. Seitz,[14] T.-A. Shibata,[24] M. Stahl,[13] M. Statera,[10] E. Steffens,[9] J. J. M. Steijger,[18] F. Stinzing,[9] S. Taroian,[27] A. Terkulov,[17] R. Truty,[15] A. Trzcinski,[26] M. Tytgat,[12] Y. Van Haarlem,[12] C. Van Hulse,[4,12] D. Veretennikov,[19] V. Vikhrov,[19] I. Vilardi,[2] C. Vogel,[9] S. Wang,[3] S. Yaschenko,[6,9] Z. Ye,[6] S. Yen,[23] B. Zihlmann,[6] and P. Zupranski[26]

(HERMES Collaboration)

[1]*Physics Division, Argonne National Laboratory, Argonne, Illinois 60439-4843, USA*
[2]*Istituto Nazionale di Fisica Nucleare, Sezione di Bari, 70124 Bari, Italy*
[3]*School of Physics, Peking University, Beijing 100871, China*
[4]*Department of Theoretical Physics, University of the Basque Country UPV/EHU, 48080 Bilbao, Spain and IKERBASQUE, Basque Foundation for Science, 48011 Bilbao, Spain*
[5]*Nuclear Physics Laboratory, University of Colorado, Boulder, Colorado 80309-0390, USA*
[6]*DESY, 22603 Hamburg, Germany*
[7]*DESY, 15738 Zeuthen, Germany*
[8]*Joint Institute for Nuclear Research, 141980 Dubna, Russia*
[9]*Physikalisches Institut, Universität Erlangen-Nürnberg, 91058 Erlangen, Germany*
[10]*Istituto Nazionale di Fisica Nucleare, Sezione di Ferrara and Dipartimento di Fisica e Scienze della Terra, Università di Ferrara, 44122 Ferrara, Italy*
[11]*Istituto Nazionale di Fisica Nucleare, Laboratori Nazionali di Frascati, 00044 Frascati, Italy*
[12]*Department of Physics and Astronomy, Ghent University, 9000 Gent, Belgium*
[13]*II. Physikalisches Institut, Justus-Liebig Universität Gießen, 35392 Gießen, Germany*
[14]*SUPA, School of Physics and Astronomy, University of Glasgow, Glasgow G12 8QQ, United Kingdom*
[15]*Department of Physics, University of Illinois, Urbana, Illinois 61801-3080, USA*
[16]*Randall Laboratory of Physics, University of Michigan, Ann Arbor, Michigan 48109-1040, USA*
[17]*Lebedev Physical Institute, 117924 Moscow, Russia*
[18]*National Institute for Subatomic Physics (Nikhef), 1009 DB Amsterdam, The Netherlands*
[19]*B.P. Konstantinov Petersburg Nuclear Physics Institute, Gatchina, 188300 Leningrad region, Russia*
[20]*Institute for High Energy Physics, Protvino, 142281 Moscow region, Russia*
[21]*Institut für Theoretische Physik, Universität Regensburg, 93040 Regensburg, Germany*
[22]*Istituto Nazionale di Fisica Nucleare, Sezione di Roma, Gruppo Collegato Sanità and Istituto Superiore di Sanità, 00161 Roma, Italy*
[23]*TRIUMF, Vancouver, British Columbia V6T 2A3, Canada*
[24]*Department of Physics, Tokyo Institute of Technology, Tokyo 152, Japan*
[25]*Department of Physics and Astronomy, VU University, 1081 HV Amsterdam, The Netherlands*
[26]*National Centre for Nuclear Research, 00-689 Warsaw, Poland*
[27]*Yerevan Physics Institute, 375036 Yerevan, Armenia*

(Received 30 December 2013; revised manuscript received 13 May 2014; published 30 May 2014)

[*]Present address: Brookhaven National Laboratory, Upton, New York 11772-5000, USA.

An earlier extraction from the HERMES experiment of the polarization-averaged parton distribution of strange quarks in the nucleon has been reevaluated using final data on the multiplicities of charged kaons in semi-inclusive deep-inelastic scattering obtained with a kinematically more comprehensive method of correcting for experimental effects. General features of the distribution are confirmed, but the rise at low x is less pronounced than previously reported.

DOI: 10.1103/PhysRevD.89.097101 PACS numbers: 13.60.-r, 13.88.+e, 14.20.Dh, 14.65.-q

The parton distribution functions (PDFs) of the strange quarks in the nucleon describe important features of the structure of the quark sea and constrain models of its origin [1–4]. In addition, the strangeness content of the nucleon is of interest because of its impact on calculations of short-distance processes at high energies [5] and also in view of recent ATLAS results [6], which suggest that at small x it could be substantially larger than previously assumed. In 2008 HERMES published the results of the extraction of the momentum and helicity density distributions of the strange sea in the nucleon from charged-kaon production in deep-inelastic scattering (DIS) on the deuteron [7]. The shape of the polarization-averaged distribution in x, where x is the dimensionless Bjorken scaling variable, was observed to be softer than that of the average of the $\bar{u}$ and $\bar{d}$ quarks. The helicity distribution was found to be compatible with zero in the region of measurement $0.02 < x < 0.60$.

HERMES has finalized the extraction of multiplicities for each charged state of $\pi^{\pm}$ and $K^{\pm}$ [8]. In the extraction, the correction for acceptance, kinematic smearing, losses due to decay in flight and secondary strong interactions, and radiative effects is accomplished by means of a smearing matrix which is generated with a Monte Carlo simulation. The procedure is described in detail in Ref. [8]. The data of Ref. [7] were obtained by carrying out the unfolding to correct for these effects in only one dimension, x. Further study of the unfolding procedure has revealed that using a multidimensional unfolding in x, z, and $P_{h\perp}$ results in significant changes in the final multiplicities. Here $z \equiv E_h/\nu$ with ν and E_h the energies of the virtual photon and the detected hadron in the target rest frame, respectively, and $P_{h\perp}$ the transverse momentum of the hadron with respect to the virtual-photon direction. The results for the final multiplicities [8] were obtained with this improvement and with the elimination of a requirement, used in earlier extractions, that the hadrons have momenta greater than 2 GeV. In practice, multiplicities are not defined with such a limit on the integration over the hadron momentum. The purpose of this brief note is to update the extraction of the strange-quark PDF $S(x) \equiv s(x) + \bar{s}(x)$ by employing the final HERMES multiplicities obtained by this advanced analysis. The extraction is carried out in leading logarithmic order (LO) in the strong coupling constant of quantum chromodynamics. While a next-to-leading order (NLO) extraction would be preferred, such a procedure using semi-inclusive DIS data is not currently available. However, because of the wide interest in shape and magnitude of $S(x)$, a LO extraction is an important first step.

In the isoscalar method used in the HERMES measurement, the distribution in x of the strange-quark sea is extracted from the spin-averaged kaon, $K \equiv K^+ + K^-$, multiplicity for the DIS of positrons/electrons by a deuteron target [7]. For the isoscalar deuteron, in LO this observable depends on the PDFs $S(x)$ and $Q(x) \equiv u(x) + \bar{u}(x) + d(x) + \bar{d}(x)$. Technical details of the experiment and the principles of the procedure for extracting the density distributions for these quantities are presented in Ref. [7]. The extracted kaon multiplicity is shown in Fig. 1 as a function of x at the corresponding average Q^2 of each bin.

The multiplicity presented in Fig. 1 is the starting point for the extraction of $S(x, Q^2)$ and can be used in the future, e.g., for NLO analyses. Here we update the extraction of $S(x, Q^2)$ which is based on a number of simplifying assumptions, i.e., LO and leading twist, as well as on fixing the fragmentation functions and PDFs to a specific set. As in the analysis reported earlier, both $S(x, Q^2)$ and

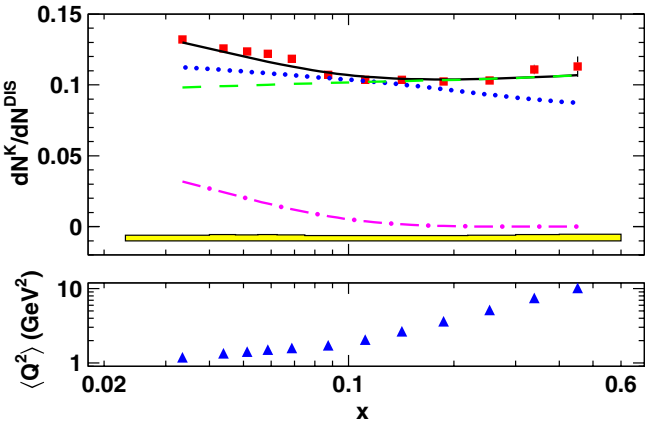

FIG. 1 (color online). The multiplicity of charged kaons in semi-inclusive DIS from a deuterium target, as a function of Bjorken x. The continuous curve is calculated from the strange-quark contribution taken from the fit in Fig. 3, together with the nonstrange contribution as extracted from the high-x multiplicity data (see text). The green dashed (magenta dash-dotted) curve shows separately the nonstrange- (strange-) quark contribution to the multiplicity for that fit. The blue-dotted curve is the LO prediction obtained with CTEQ6L PDFs and fragmentation functions from [9]. The values of $\langle Q^2 \rangle$ for each x bin are shown in the lower panel. The band represents systematic uncertainties.

the quantity $\int \mathcal{D}_S^K(z,\mathrm{Q}^2)dz$ are taken as unknown, and the analysis is carried out extracting their product. Here, $\int \mathcal{D}_S^K(z,\mathrm{Q}^2)dz$ is the integral over the measured region of z of the fragmentation function describing the number density of charged kaons from a struck quark of flavor S, with $\mathcal{D}_S^K(z) \equiv 2\mathcal{D}_s^K(z)$ by charge conjugation symmetry. The relationship between this product and the kaon multiplicity is given in LO by [7]

$$\frac{dN^K(x,\mathrm{Q}^2)}{dN^{\mathrm{DIS}}(x,\mathrm{Q}^2)} = \frac{Q(x,\mathrm{Q}^2)\int \mathcal{D}_Q^K(z,\mathrm{Q}^2)dz + S(x,\mathrm{Q}^2)\int \mathcal{D}_S^K(z,\mathrm{Q}^2)dz}{5Q(x,\mathrm{Q}^2) + 2S(x,\mathrm{Q}^2)}. \quad (1)$$

An absence of x dependence shown by the HERMES data above $x > 0.1$ requires that $d[S(x))/Q(x)]/dx$ vanish. This indicates that either $S(x) = 0$ or $S(x) = kQ(x)$ where k is a constant. $S(x)$ is not expected to have the same shape as $Q(x)$, and all PDF reference data sets published to date are consistent with this expectation. Therefore for $x > 0.1$ it is concluded that $S(x,\mathrm{Q}^2) \approx 0$.

In the limit $S(x,\mathrm{Q}^2) \to 0$, for a deuteron target the multiplicity $dN^K(x,\mathrm{Q}^2)/dN^{\mathrm{DIS}}(x,\mathrm{Q}^2) = \int \mathcal{D}_Q^K(z,\mathrm{Q}^2)dz/5$ [see Eq. (1)]. For $x > 0.1$ the multiplicity measured by HERMES is almost constant at a value of about 0.1. The value of the multiplicity throughout this region provides a direct estimate of $\int \mathcal{D}_Q^K(z,\mathrm{Q}^2)dz$. To account for any residual dependence on Q^2 or, because of the correlation between x and Q^2, equivalently on x, a first-degree polynomial was fitted to the multiplicity for $x > 0.1$ yielding the result that $dN^K(x,\mathrm{Q}^2)/dN^{\mathrm{DIS}}(x,\mathrm{Q}^2) = (0.102 \pm 0.002) + (0.013 \pm 0.010)x$, as shown by the green dashed curve in Fig. 1. In the region near $x = 0.13$, where $\mathrm{Q}^2 \approx 2.5$ GeV^2, this fit gives the result $\int_{0.2}^{0.8} \mathcal{D}_Q^K(z,\mathrm{Q}^2)dz = 0.514 \pm 0.010$, compared to the value 0.435 ± 0.044 obtained for $\mathrm{Q}^2 = 2.5$ GeV^2 from a global analysis of fragmentation functions [9]. The weak x dependence obtained in the fit is consistent with the Q^2 dependence exhibited by the results of the global analysis.

To assess the impact of the more accurate estimate of $\int \mathcal{D}_Q^K(z,\mathrm{Q}^2)dz$ resulting from the HERMES data, an extraction of $S(x,Q^2)$ was made using the fragmentation functions from the global analysis of [9]. The results, presented in Fig. 2, have an $xS(x,Q^2)$ with large uncertainties in the high-x region, and demonstrate the importance of a more precise value for $\int \mathcal{D}_Q^K(z,\mathrm{Q}^2)dz$ as is that extracted from the analysis reported here.

The extracted quantity $\int_{0.2}^{0.8} \mathcal{D}_Q^K(z,\mathrm{Q}^2)dz$ was used together with values of $Q(x,\mathrm{Q}^2)$ from CTEQ6L [11] and the measured multiplicity to obtain the product $S(x,\mathrm{Q}^2)\int \mathcal{D}_S^K(z,\mathrm{Q}^2)dz$. As in Ref. [7], the contribution of the strange quarks to the denominator in Eq. (1) was initially neglected leading to

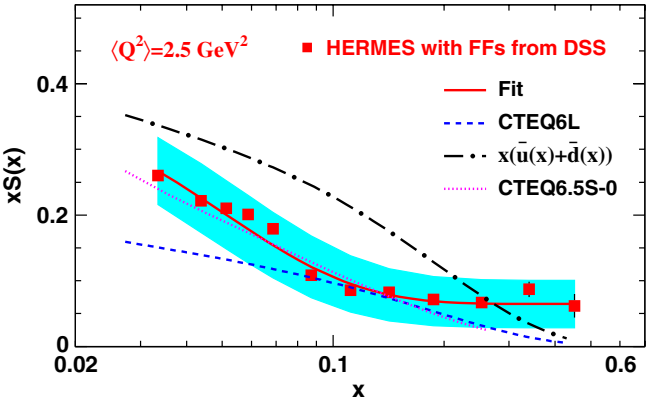

FIG. 2 (color online). The strange-parton distribution $xS(x,\mathrm{Q}^2)$ from the measured HERMES multiplicity for charged kaons evolved to $\mathrm{Q}^2 = 2.5$ GeV^2 using the compilation of fragmentation functions (FFs) from [9] (DSS). The solid curve is a three-parameter fit to the data, the dashed curve gives $xS(x)$ from CTEQ6L, and the dot-dash curve is the sum of light antiquarks from CTEQ6L. The dotted curve is from CTEQ6.5S-0, a PDF reference set [10] in which the shape of $xS(x)$ has not been constrained. The band containing the experimental points represents the fully correlated systematic uncertainties arising from the imprecision of $\int \mathcal{D}_Q^K(z,\mathrm{Q}^2)dz$.

$$S(x,\mathrm{Q}^2)\int \mathcal{D}_S^K(z,\mathrm{Q}^2)dz \simeq Q(x,\mathrm{Q}^2)\left[5\frac{dN^K(x,\mathrm{Q}^2)}{dN^{\mathrm{DIS}}(x,\mathrm{Q}^2)} - \int \mathcal{D}_Q^K(z,\mathrm{Q}^2)dz\right]. \quad (2)$$

A small iterative correction was then made to account for the neglect of this term.

The result for the product $S(x,\mathrm{Q}^2)\int \mathcal{D}_S^K(z,\mathrm{Q}^2)dz$ together with a fit of the form $x^{-a_1}e^{-x/a_2}(1-x)$ are shown in Fig. 3. In the region $x < 0.1$ the values of the product are

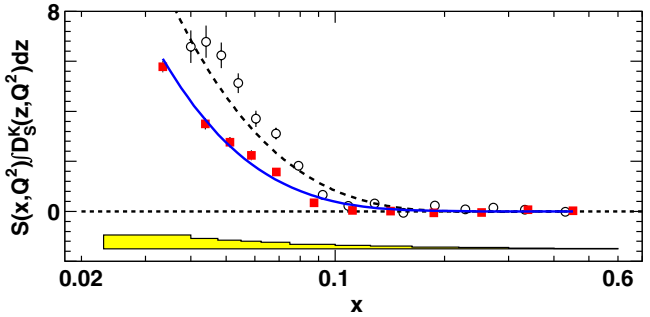

FIG. 3 (color online). The product, $S(x,\mathrm{Q}^2)\int \mathcal{D}_S^K(z,\mathrm{Q}^2)dz$, of the strange-quark PDF and the integral of the fragmentation function for strange quarks (squares) obtained from the measured HERMES multiplicity for charged kaons at the $\langle \mathrm{Q}^2 \rangle$ for each bin. The solid curve is a least-squares fit with the result $f(x) = x^{-0.834\pm0.019}e^{-x/(0.0337\pm0.0014)}(1-x)$. The band represents propagated experimental systematic uncertainties. The open points and the dashed curve show the data and fit published previously in Ref. [7].

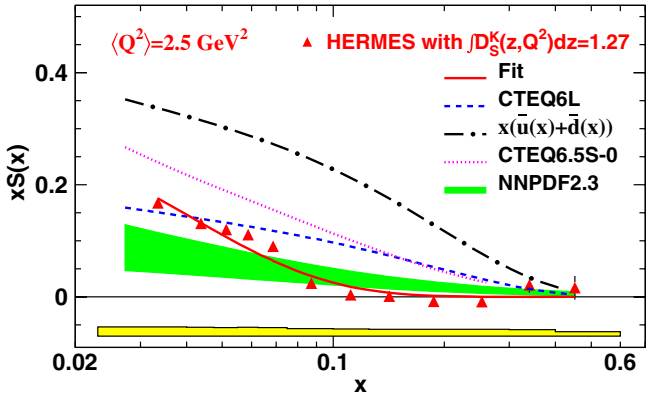

FIG. 4 (color online). The strange-parton distribution $xS(x, Q^2)$ from the measured HERMES multiplicity for charged kaons evolved to $Q^2 = 2.5$ GeV^2 assuming $\int \mathcal{D}_S^K(z, Q^2)dz = 1.27$. The solid curve is a two-parameter fit with $S(x) = [\int \mathcal{D}_S^K(z, Q^2)dz]^{-1} \times x^{-0.867\pm0.019} e^{-x/(0.0331\pm0.0014)}(1-x)$. The dashed, dot-dash, dotted curves are as given in Fig. 2. The broad band is the $\pm 1\sigma$ zone of allowed values predicted by the neural network (NNPDF2.3) reference set [14]. The band at the bottom represents the propagated experimental systematic uncertainties. A scale uncertainty of approximately 10% coming from the precision of $\int \mathcal{D}_S^K(z, Q^2)dz$ is not shown.

substantially smaller than those reported previously [7]. This fit leads to the solid curve shown in Fig. 1. The use of the most recent NNPDF2.3LO reference PDF set [12] in place of the CTEQ6L PDFs does not alter significantly the results of the extraction.

In order to compare the distribution of $S(x, Q^2)$ with the average of those of the nonstrange quarks, the HERMES result for $S(x, Q^2)\int \mathcal{D}_S^K(z, Q^2)dz$ has been evolved to $Q^2 = 2.5$ GeV^2. The Q^2 evolution factors are taken from CTEQ6L and from the fragmentation function compilation given in Ref. [9]. Corrections to the evolution due to higher-twist contributions are assumed to be negligible, because higher-twist effects are expected to be significant only for larger values of x [13], where the extracted distribution of $xS(x, Q^2)$ vanishes. The distribution of $xS(x, Q^2)$ was obtained from $S(x, Q^2)\int \mathcal{D}_S^K(z, Q^2)dz$ by dividing it by $\int \mathcal{D}_S^K(z, Q^2)dz = 1.27$, the value at $Q^2 = 2.5$ GeV^2 given in [9]. The uncertainty on $\int \mathcal{D}_S^K(z, Q^2)dz$ enters only as a scale uncertainty in the extracted $xS(x, Q^2)$. The results are presented in Fig. 4.

Due to the anticorrelation of strange and nonstrange kaon fragmentation functions in a global analysis, a proper consideration of the nonstrange kaon fragmentation function obtained here may lead to a considerably smaller strange kaon fragmentation function. Such a revision can be expected in the next global analysis, with the result that the strange distribution as extracted here may increase.

As in the earlier extraction, the normalization of the HERMES points is determined by the value of $\int \mathcal{D}_S^K(z, Q^2)dz$ assumed. The values of the extracted distribution of $S(x, Q^2)$ are smaller than those reported in Ref. [7]. But still, the qualitative features of the shape of $xS(x, Q^2)$ are strikingly different from the shape of $xS(x, Q^2)$ obtained with CTEQ6L and other global QCD fits of LO PDFs as well as that of the sum of the light antiquarks. The absence of strength above $x \approx 0.1$ is clearly discrepant with CTEQ6L. While, in principle, the new values for the kaon multiplicities and fragmentation integrals reported here could significantly alter the results of the strange-quark helicity-distribution extraction reported in Ref. [7], in fact, their use produces no significant change in the helicity distribution reported there.

In conclusion, a new extraction of the multiplicities for charged kaons in DIS has been made and the extraction of the distribution of strange quarks in the nucleon has been reevaluated using these new data. In the measured range of x, the strength of the polarization-averaged PDF $S(x, Q^2)$ is, under the same assumptions, substantially less than reported in [7], but the shape is similar, and the momentum density is softer than that determined from the analysis of other experiments.

ACKNOWLEDGEMENTS

We warmly thank Juan Rojo for his efforts in generating an unpublished NNPDF2.3LO PDF data set that includes the kinematic region of the HERMES experiment, and we gratefully acknowledge the DESY management for its support, the staff at DESY and the collaborating institutions for their significant effort, and our national funding agencies for financial support.

[1] J. Bjorken, Phys. Rev. **179**, 1547 (1969).
[2] R. Feynman, *Photon-Hadron Interactions* (Benjamin, New York, 1973).
[3] M. Glück, R. Godbole, and E. Reya, Z. Phys. C **41**, 667 (1989).
[4] M. Glück, E. Reya, and A. Vogt, Z. Phys. C **53**, 127 (1992).
[5] A. Kusina, T. Stavreva, S. Berge, F. I. Olness, I. Schienbein, K. Kovařík, T. Ježo, J. Y. Yu, and K. Park, Phys. Rev. D **85**, 094028 (2012).
[6] G. Aad *et al.* (ATLAS Collaboration), Phys. Rev. Lett. **109**, 012001 (2012).

[7] A. Airapetian *et al.* (HERMES Collaboration), Phys. Lett. B **666**, 446 (2008).
[8] A. Airapetian *et al.* (HERMES Collaboration), Phys. Rev. D **87**, 074029 (2013).
[9] D. de Florian, R. Sassot, and M. Stratmann, Phys. Rev. D **75**, 114010 (2007).
[10] H.-L. Lai, P. Nadolsky, J. Pumplin, D. Stump, W.-K. Tung, and C.-P. Yuan, J. High Energy Phys. 04 (2007) 089.
[11] J. Pumplin, D. R. Stump, J. Huston, H.-L. Lai, P. Nadolsky, and W.-K. Tung, J. High Energy Phys. 07 (2002) 012.
[12] J. Rojo (NNPDF Collaboration) (private communication).
[13] A. D. Martin, R. G. Roberts, W. J. Stirling, and R. S. Thorne, Phys. Lett. B **443**, 301 (1998).
[14] R. D. Ball, V. Bertone, F. Cerutti, L. Del Debbio, S. Forte, A. Guffanti, J. I. Latorre, J. Rojo, and M. Ubiali (NNPDF Collaboration), Nucl. Phys. **B855**, 153 (2012).